ELSEVIER

Biochimica et Biophysica Acta 1410 (1999) 19–31

BIOCHIMICA ET BIOPHYSICA ACTA
BBA

Interaction of photosynthetic pigments with various organic solvents

Magnetic circular dichroism approach and application to chlorosomes

Mitsuo Umetsu [a, b], Zheng-Yu Wang [a, b], Masayuki Kobayashi [a, b], Tsunenori Nozawa [a, b, *]

[a] *Department of Biomolecular Engineering, Graduate School of Engineering, Tohoku University, Aobayama 07, Aoba-ku, Sendai 980-8579, Japan*

[b] *Center for Interdisciplinary Research, Tohoku University, Sendai 980-8579, Japan*

Received 14 September 1998; received in revised form 16 November 1998; accepted 19 November 1998

Abstract

Magnetic circular dichroism (MCD) and absorption spectra have been measured on three intact photosynthetic pigments with the chlorin ring as macrocycle: chlorophyll *a*, bacteriochlorophyll *c* and *d*, in various hydrophilic organic solvents. The MCD intensity of a Q_y(0-0) transition for the Mg chlorin derivative was sensitive to the coordination state of the central Mg atom by the solvent molecules. The coordination number has been characterized in terms of the relationship between the ratio of Q_y(0-0) MCD intensity to its dipole strength (B/D) and the difference in energies of Q_x(0-0) and Q_y(0-0) transitions. This relationship depends not only on the coordination number of the magnesium (Mg) atom but also on the coordination interaction of the solvent molecules to the Mg atom, and can clarify the spectroscopic change of chlorosomes by alcohol treatment. We propose that the correlation between the MCD intensity of Q_y(0-0) transition and the energy difference can be used as a new measure for determining the coordination number of the Mg atom and for estimating the interaction strength of the Mg atom with solvent molecules.

Keywords: Magnetic circular dichroism; Bacteriochlorophyll *c*; Coordination state; Chlorosome; Alcohol treatment

1. Introduction

Photosynthetic pigments perform several important roles in the light-harvesting and energy-transducing systems in green plants and bacteria [1,2]. These pigments usually function in various aggregated forms through pigment/pigment or pigment/protein interactions. The organization of the photosynthetic pigments in vivo in both the antenna and reaction center is crucial to our understanding of the mechanism of photosynthesis. For this reason, the complexation phenomena of photosynthesis-related pigment molecules in various environments have been extensively investigated using a variety of spectroscopic methods, including infrared [3,4], absorption [5,6], resonance Raman [7–14], fluorescence and magnetic circular dichroism (MCD) [15–19]. The Raman spectra in the 1620–1510 cm^{-1} region were well used to distinguish between the five- and six-

* Corresponding author, at address a. Fax: +81 (22) 2177279; E-mail: nozawa@biophys.che.tohoku.ac.jp

0005-2728/99/$ – see front matter
PII: S0005-2728(98)00170-4

coordinate species for chlorophyll (Chl) *a* in various organic solvents [8]. The visible absorption spectra in the 560–620 nm were also used to differentiate the coordination state of the central magnesium (Mg) atom for bacteriochlorophyll (BChl) *a* [20]. The Q_x band of five-coordinated Mg species was found to appear at near 580 nm, whereas that of six-coordinated Mg species was red-shifted to about 610 nm. The coordination behavior for highly symmetric metalloporphyrins has been studied with MCD [17]. The relative intensity of the Soret (B_x 350–500 nm) and the Q_y bands differed depending on the coordination number.

In this study, we are concerned with absorption and MCD spectral data for three photosynthetic pigments: Chl *a*, BChl *c* and *d*, all having the chlorin ring as macrocycle. Chl *a* is the principal photoreceptor in the photosynthetic units of all organisms that carry out photosynthesis with evolution of molecular oxygen. BChl *c* and *d* can be regarded as pyrochlorophylls and are major photosynthetic pigments found in green sulfur bacteria. They function to absorb light energy, which is then transferred to the adjacent photosynthetic membrane. The major difference in structure of BChl *c* and *d* is the extra methylation attached to the 20-carbon (BChl *c* only, Fig. 1), whereas the structural differences between Chl *a* and BChl *c*, *d* are probably the existence of a 3^1-hydroxyl group and lack of the 13^2-carboxymethyl substituent for BChl *c* and *d*. While the macrocycle of the three molecules closely resembles the porphyrin ring, the additional five-membered ring attached to pyrrole III and the reduction of pyrrole IV serve to reduce the symmetry from the D_{4h} of many porphyrins. According to Gouterman's four-orbital theory [21], the structural perturbation lifts degeneracy of the two lowest unoccupied molecular orbitals (LUMOs), and the two highest occupied molecular orbitals (HOMOs) are originally non-degenerate. As a result, the MCD spectra of such molecules are dominated by the Faraday *B*-term, in contrast to the D_{4h} porphyrins for which the Faraday *A*-term is considered the major contribution [22]. The *B*-term arises from the mixing of two or more non-degenerate states of *x*- and *y*-polarization by the external magnetic field and usually show an absorption band with either positive or negative sign [23–25]. The intensity and signs of MCD are known to be very sensitive to the changes in the electronic state of chromophores and these are practically useful for detecting very weak electronic transitions (e.g., chlorin Q_x band) as the transitions will be significantly enhanced by mixing with closely related states of *x*- and *y*-polarization.

Chlorosomes are the major light-harvesting apparatus in green photosynthetic bacteria and are attached to the cytoplasmic side of the inner cell membrane [26,27]. Chlorosomes contain bacteriochlorophyll *c*, more than 50% (by weight) as the major component, and also contain carotenoids, lipids, proteins and a small amount of BChl *a*. At present it is a general consensus that BChl *c* is self-aggregated in chlorosomes, and that protein does not play a fundamental role in BChl *c* aggregation in chlorosomes [28–30]. A relatively large number of studies on spectroscopic changes of chlorosomes by hexanol treatment have been reported. The absorption, circular dichroism and MCD spectra changed to the same monomeric form as that of isolated BChl *c* in hydrophilic organic solvents [31]. However, these spectroscopic changes are not elucidated distinctly. Recently, we have reported an empirical correlation between the aggregation number for the pigments both in vivo and in vitro with the MCD intensity [18]. It was found that for chlorin and bacteriochlorin dimers the ratio of Q_y intensity of MCD spectra to the dipole strength (*B*/*D*) obtained from absorption spectra is about half that for monomer, if the coordination number of the Mg atom remains unchanged. But no correlation was observed when the central Mg atom has different coordination numbers for monomer and dimer. We describe, in this paper, the absorption and MCD spectra of Mg chlorin derivatives in various hydrophilic organic solvents. Detailed deconvolution calculations were carried out on these data using the strong magnetic moments observed for Q_x and Q_y bands in the MCD spectra. We are able to correlate the coordination number and interaction with deconvoluted transition components. This correlation provides information not only on the coordination number for the central metal but also on the interaction with deconvoluted transition components, and further indicates that the spectroscopic changes of chlorosomes by hexanol treatment are due to the ligation of hexanol molecules to the Mg atom of BChl *c*.

2. Experimental

2.1. Materials

Chl *a* was obtained as previously reported [32]. BChl *c* was extracted from dry cells of the thermophilic green photosynthetic bacterium *Chlorobium tepidum* with methanol and purified as described previously [33]. BChl *c* used in this study was (3^1R)-8-ethyl-12-ethyl farnesyl BChl *c* (Fig. 1). BChl *d* was extracted from *Chlorobium limicola* using a method similar to that of Kobayashi et al. [18]. All of the purified pigments were characterized by NMR. Organic solvents were of spectroscopic grade and molecular sieves (3A) were used to remove trace water. Chlorosomes were extracted as described previously [31].

2.2. Instruments and spectroscopic methods

Absorption spectra were recorded on a Beckman DU-640 spectrophotometer with a 1 cm quartz cuvette. MCD spectra were measured on a Jasco J-720w spectropolarimeter with a 1 cm quartz cuvette. The conditions of MCD measurement were as follows: band width 1.0 nm, resolution 0.5 nm, response 1 s, scan speed 20 nm/min and external magnetic field 1.5 T.

Pigments were dissolved in diethyl ether, acetone, THF, dioxane, pyridine and alcohols. Three alcohols (methanol, ethanol and 1-*n*-hexanol) and THF were titrated in 20 mM potassium phosphate solutions of chlorosomes to change spectra of chlorosomes to monomeric ones. For hexanol treatment, the saturated buffer (59 mM) was used, and other organic solvent's concentrations were as follows: methanol: 17 M, ethanol: 9.5 M, THF: 4 M. Extinction coefficients used for Chl *a* were 8.51×10^4 l/(mole×cm) in diethyl ether and 7.69×10^4 l/(mole×cm) in pyridine [34]. For BChl *c* and *d*, the extinction coefficients were calculated to be 7.3×10^4 l/(mole×cm) for BChl *c* and 8.83×10^4 l/(mole×cm) for BChl *d* in diethyl ether, based on values of the literature [35].

The deconvolutions of absorption and MCD spectra were performed using the non-linear curve fitting tool of a software GRAMS/32 V5.0 (Galactic) according to the following criteria: (1) each pair of the absorption and MCD spectra was deconvoluted into the same number of components; (2) each pair of associated components in the absorption and MCD spectra was constrained to give the same band center and band width parameters; (3) a mixed Gaussian-Lorentzian function was used to fit each component and the weight factors were allowed to vary for different components but keep the same value for the same component of the associated absorption and MCD spectra; (4) the deconvolution continued until χ^2 (the sum of squares of the deviations normalized by the variance of count) attained less than three.

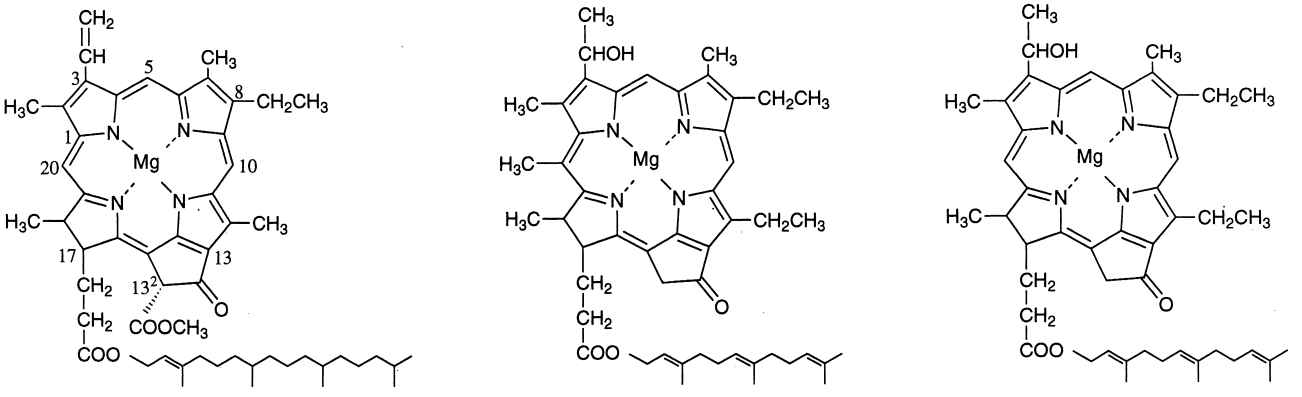

(a) Chlorophyll *a* (Chl *a*) (b) Bacteriochlorophyll *c* (BChl *c*) (c) Bacteriochlorophyll *d* (BChl *d*)

Fig. 1. Molecular structures of Chl *a*, BChl *c* and BChl *d*.

3. Results

3.1. Absorption and MCD spectra

Fig. 2 shows the absorption and MCD spectra of Chl *a* in diethyl ether and pyridine. It is well known that Chl *a* forms five-coordinate species in diethyl ether and six-coordinate species in pyridine [8,12,14,20]. The spectra observed in diethyl ether were essentially the same as those reported previously [15,18], where the strong Q_y(0-0) transition appeared at 660 nm. There are several bands in the 520–620 nm region which can be assigned to Q_x and vibrational transitions. Whereas in pyridine, overall spectra shifted about 10 nm to the long wavelength and the spectral shape for the absorption was about the same except that the small peaks in 550–640 nm were less resolved. However, notable differences in the MCD spectrum were observed in the visible region. The intensities of the positive Q_y(0-0) band (670 nm) and the negative 638 nm band increased significantly in comparison with the corresponding bands in diethyl ether (660 nm and 617 nm, respectively). Consequently, the intensities for the two negative bands (638 nm and 599 nm) were reversed as the intensity for the 599 nm band remained almost unchanged compared with that of the corresponding band in diethyl ether (577 nm).

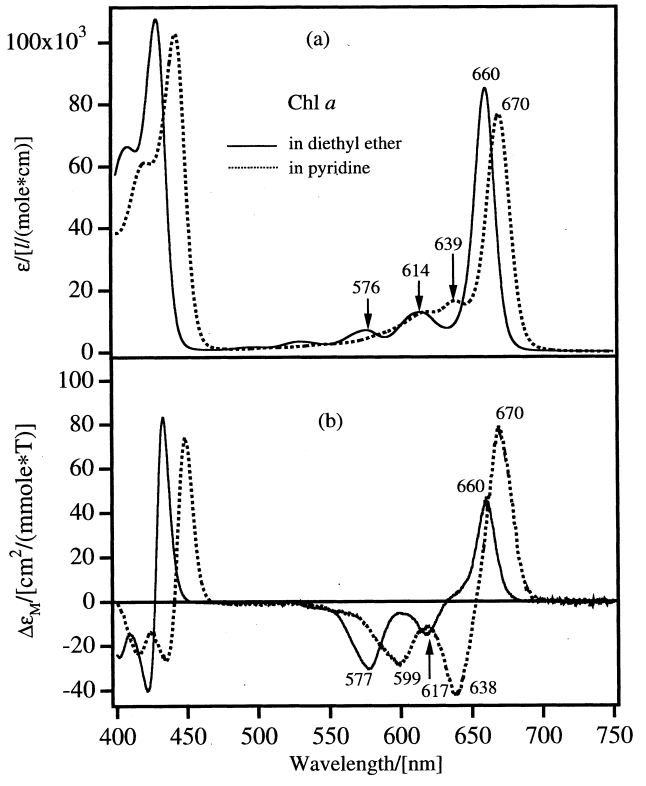

Fig. 2. Absorption (a) and MCD (b) spectra of Chl *a* in diethyl ether (solid lines) and pyridine (dotted lines). Concentrations were 1.17×10^{-5} mol/l in diethyl ether and 1.12×10^{-5} mol/l in pyridine, respectively.

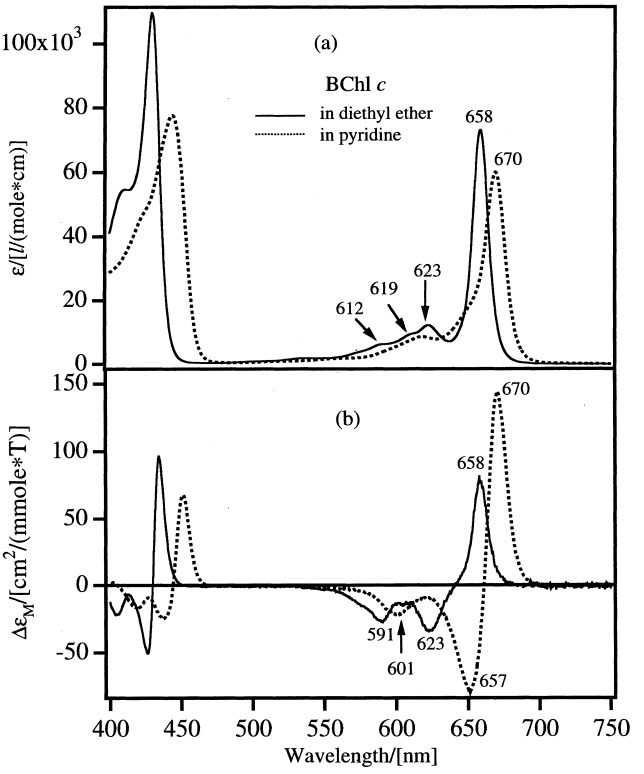

Fig. 3. Absorption (a) and MCD (b) spectra of BChl *c* in diethyl ether (solid lines) and pyridine (dotted lines). Concentrations were 7.8×10^{-6} mol/l in diethyl ether and 1.5×10^{-5} mol/l in pyridine, respectively.

Fig. 3 shows the absorption and MCD spectra of BChl *c* in diethyl ether and pyridine. Overall, the spectra were similar to those observed for Chl *a*. Beside the spectra given here, we have measured for other solvents, such as, acetone, THF, dioxane, methanol and ethanol. Again, the MCD spectra in the long wavelength region were shown to be very sensitive to the solvents used. From the MCD spectra of Fig. 3, the most pronounced feature can be typically characterized by a marked increase in the intensities of the positive Q_y(0-0) band (670 nm) and the negative 657 nm band with a large red-shift for the 657 nm band (34 nm) in pyridine relative to those

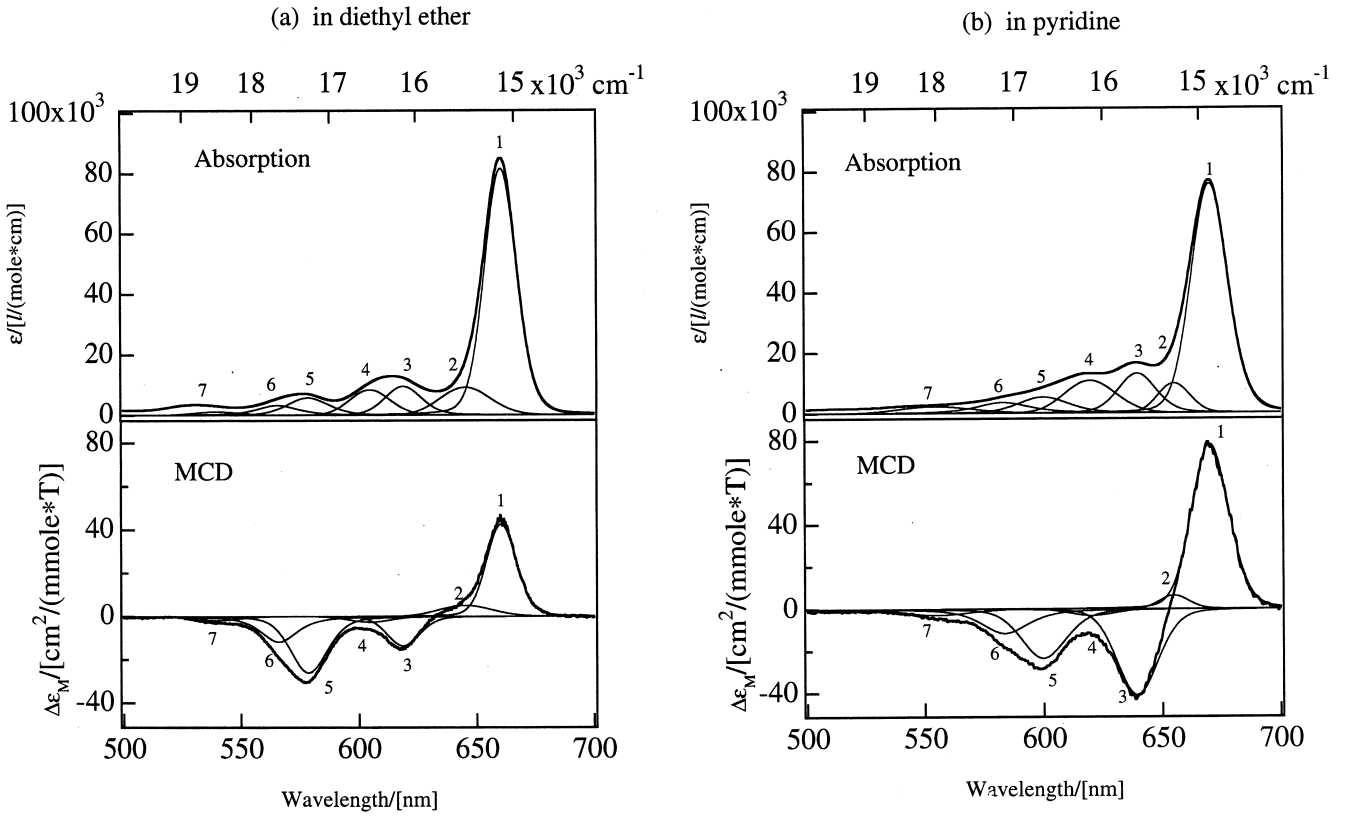

Fig. 4. Deconvolution of the absorption and MCD spectra of Chl *a*, (a) in diethyl ether and (b) in pyridine.

in diethyl ether. Different from Chl *a*, the intensities of the two negative bands at 623 nm and 591 nm in diethyl ether were reversed for BChl *c*. Since it is known that both Chl *a* and BChl *c* form five-coordinate species in diethyl ether and six-coordinate species in pyridine, the increase in intensities of Q_y(0-0) and the first negative MCD bands may correspond to a change in the coordination number from five to six. The absorption and MCD spectra for BChl *d* were essentially the same as those from Chl *a* except that peak positions shifted about 10 nm to the short wavelength side (data not shown).

3.2. Deconvolution of the absorption and MCD spectra

The MCD measurements on the three photosynthetic pigments indicated that the spectra in the visible region clearly vary with the solvents used, implying that the spectral behavior may correlate with the interaction between the pigment and the solvent molecules, or, in other words, the coordination states, because no aggregation between the pigment molecules can occur in these solvents. In order to make a quantitative argument, we have performed a simultaneous deconvolution on the absorption and MCD spectra. In the calculations, the same parameters were used to fit pairs of associated components in the absorption and MCD spectra, i.e., the same number of components, the same band centers and half-widths. Fig. 4 shows the deconvolution results for Chl *a* in the visible region. For both solvents, at least seven components were required for a satisfactory fitting. The large band 1 obviously corresponds to the Q_y(0-0) transition. The relatively small band 2 was necessary in fitting the absorption spectra. The absorption peak around 614 nm for Chl *a* in diethyl ether was previously fitted by one component when only the absorption spectrum was deconvoluted [6]. We have found that at least two components were needed in order to satisfy both the absorption and MCD spectra. The two bands (3 and 4) had almost equal intensities for the absorption spectra but were quite different in the MCD activity. Table 1 summa-

Table 1
Fitting parameters for Chl *a* in diethyl ether and pyridine (in parentheses)

Band	λ (nm)	υ (cm^{-1})	ε (10^3 l/(mole×cm))	$\Delta\varepsilon_M$ (cm^2/(mmole×T))	*B*/*D* ($k\beta/cm^{-1}$)
1	660.4	15 143	81.6	42.4	52.5
	(670.1)	(14 923)	(75.7)	(78.0)	(113.2)
2	645.2	15 500	9.07	4.98	62.9
	(655.1)	(15 266)	(9.72)	(6.23)	(62.4)
3	619.0	16 155	9.42	−13.6	−140.7
	(639.4)	(15 640)	(13.0)	(−41.0)	(−372.9)
4	604.8	16 535	8.30	−2.61	−36.1
	(619.6)	(16 140)	(10.6)	(−3.22)	(−29.4)
5	578.5	17 286	5.68	−26.1	−448.5
	(600.0)	(16 668)	(5.21)	(−23.6)	(−444.0)
6	565.5	17 682	3.22	−11.8	−366.3
	(583.0)	(17 152)	(3.46)	(−11.7)	(−330.5)
7	539.9	18 526	1.12	−1.82	−159.2
	(554.6)	(18 032)	(2.21)	(−2.90)	(−127.8)

The MCD *B*-term was calculated from molar ellipticity $\Delta\varepsilon_M$ as [18]: $B = 9.836\times10^5\int_{band}\Delta\varepsilon_M(\upsilon)/\upsilon d\upsilon$, where υ is wave number. The absorption dipole strength was calculated from the extinction coefficient ε as [18]: $D = 9.1834\times10^{-3}\int_{band}\varepsilon(\upsilon)/\upsilon d\upsilon$.

rizes the fitting parameters for Chl *a* in diethyl ether and pyridine. The ratio of the MCD *B*-term to the absorption dipole strength (*B*/*D*) is listed in the last column and well reflects the observed spectral features. The absolute values of *B*/*D* in pyridine increased more than 2-fold for bands 1 and 3 compared to those in diethyl ether, but were essentially unchanged for other bands.

A similar analysis was applied to the spectra of BChl *c* and *d* except the necessity of band * as the longest wavelength band. Band * was needed to better fit the spectra of BChl *c* and *d*. Fig. 5 shows the deconvolution results of absorption and MCD spectra for BChl *c* and Table 2 lists the deconvoluted band centers and *B*/*D* values for BChl *c* in various solvents. There was a tendency that the *B*/*D* values for the relatively strong bands 1 and 3 varied markedly with solvent and this may be used for characterizing the solvent property and coordination state. Pyridine and methanol, the typical six-coordinate

Table 2
B/*D* values ($k\beta/cm^{-1}$) and band centers (nm) (in parentheses) of deconvoluted components for BChl *c* in various solvents

Band	Diethyl ether	Acetone	Ethanol	1,4-Dioxane	THF	Methanol	Pyridine
*	182.1	210.3	190.1	245.5	236.8	237.7	435.2
	(675)	(677)	(687)	(676)	(676)	(689)	(685)
1	113.4	119.5	126.2	165.4	193.5	220.7	376.9
	(659)	(661)	(666)	(660)	(662)	(669)	(670)
2	104.5	68.9	13.1	131.7	198.8	133.3	73.9
	(648)	(647)	(650)	(647)	(649)	(659)	(660)
3	−321.6	−296.4	−212.1	−420.4	−451.1	−337.1	−544.5
	(624)	(627)	(636)	(632)	(637)	(647)	(653)
4	−67.0	−32.8	−20.9	−66.4	−61.4	−35.7	−60.0
	(608)	(609)	(615)	(610)	(611)	(617)	(620)
5	−612.2	−520.8	−172.3	−529.2	−657.6	−466.6	−664.0
	(590)	(593)	(599)	(595)	(596)	(600)	(603)
6	−387.2	−255.7	−127.3	−423.4	−312.5	−353.9	−486.2
	(574)	(576)	(583)	(581)	(583)	(587)	(594)
7	−93.8	−61.7	−57.2	−43.8	−34.5	−126.1	−77.2
	(543)	(551)	(555)	(551)	(559)	(5591)	(554)

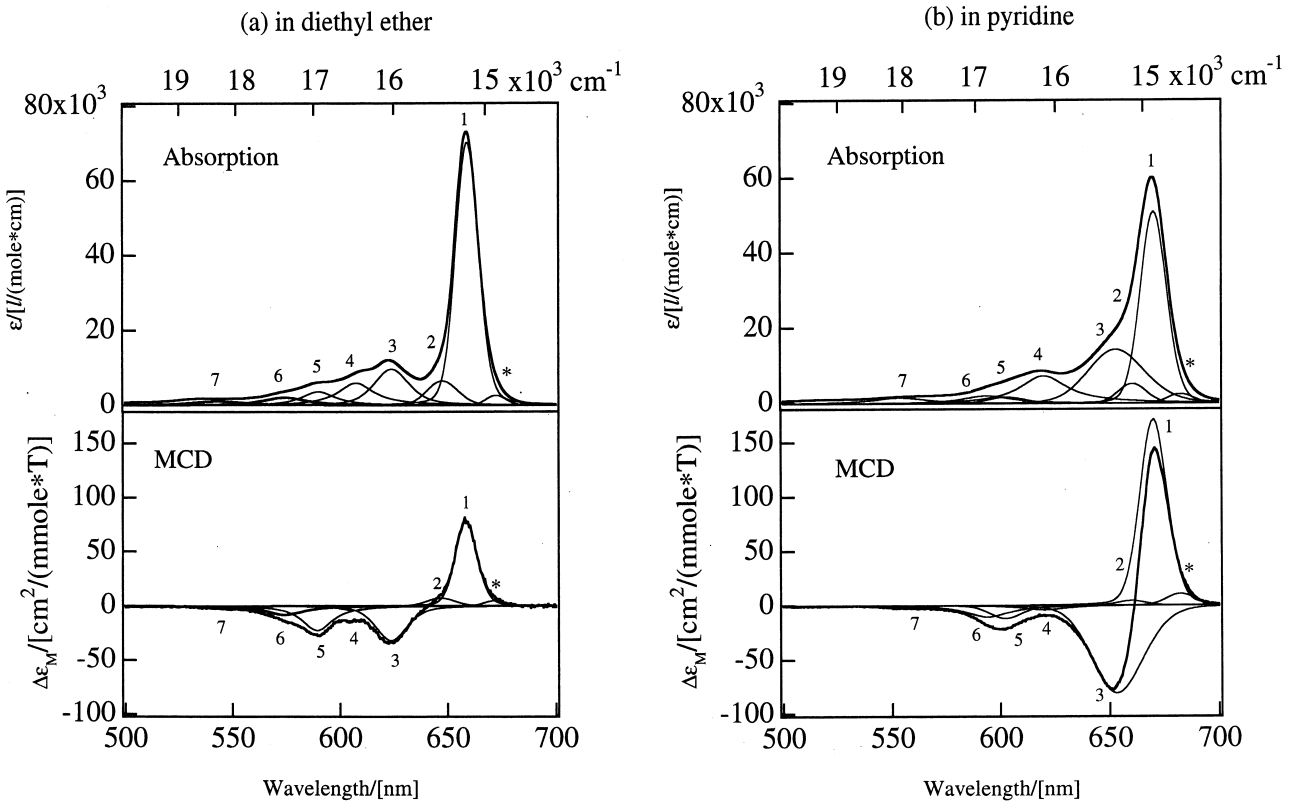

Fig. 5. Deconvolution of the absorption and MCD spectra of BChl *c*, (a) in diethyl ether and (b) in pyridine.

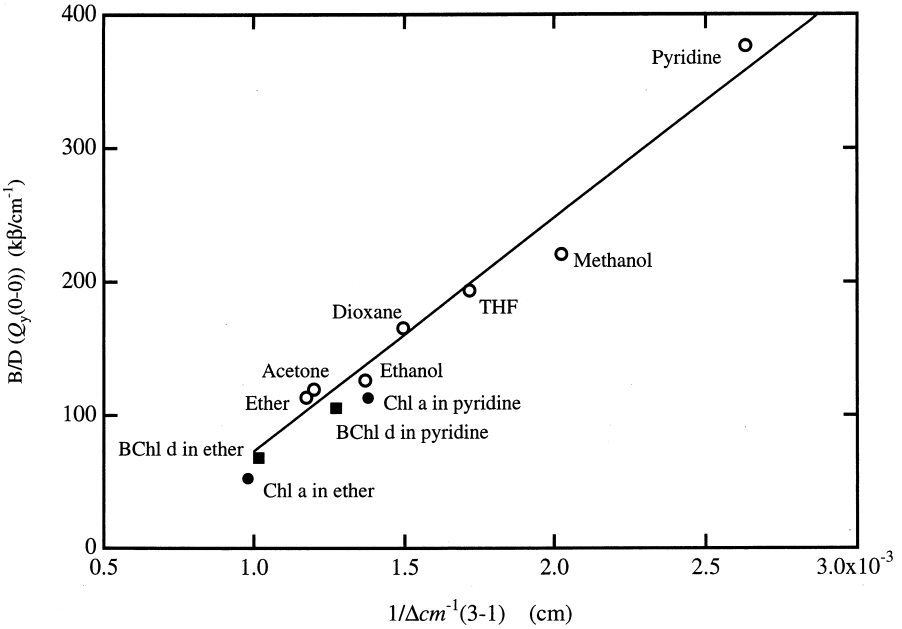

Fig. 6. Correlation between $B/D(Q_y(0\text{-}0))$ and $1/\Delta cm^{-1}(3-1)$ for BChl *c* in various solvents, where $\Delta cm^{-1}(3-1)$ represents the wave number difference between bands 3 and 1. The solid line is the least squares line for BChl *c* in organic solvents. The data for Chl *a* and BChl *d* in diethyl ether and pyridine are also plotted with closed symbols.

solvents, gave rise to large *B*/*D* values, whereas diethyl ether and acetone, known as five-coordinate solvents for BChl *c*, had relatively small *B*/*D* values. It should be pointed out that the variations of *B*/*D* for bands 2 and 4 were mainly due to a deconvolution error resulted from the low MCD intensities. Deconvolution on the absorption and MCD spectra of BChl *d* in pyridine and diethyl ether gave a result similar to that for Chl *a*.

The pronounced changes in MCD spectra of the three pigments in different solvents attracted our concern and prompted us to find out the relationship between the *B*/*D* value and interaction of pigments with the solvent molecules. Since the MCD spectra observed for these pigments are predominated by the Faraday *B*-term that originates from the mixing among non-degenerate states with mutually perpendicular polarization and are qualitatively inversely proportional to the difference in energies of these states, the *B*/*D* value for a certain band reflects a normalized effect mainly from the mixing between the neighboring transition states with *x*- and *y*-polarization. We analyzed the correlations between *B*/*D* values of Q_y(0-0) and its energy differences with other bands. Good correlation was found only for band 3 as shown in Fig. 6, whereas no essential correlations were obtained for other bands (data not shown). Therefore, it is likely that the energy difference between band 3 and Q_y(0-0) plays an important role in enhancing the MCD intensities, and the energy difference depends on both coordination number and molecular structure. This fact is also supported by the result of the MCD intensity shown in Fig. 7. When pyridine was titrated in the diethyl ether solution of BChl *c*, the MCD intensity of bands 1 and 3 became stronger. This fact may indicate a strong mixing of bands 1 (Q_y(0-0)) and 3. Considering theoretically, *x*-polarized transition should interact with Q_y(0-0) transition (band 1). According to Michl's model [23], chlorin shows an inverted MCD pattern with a positive Q_y(0-0) transition, and Q_y(0-0) and Q_x(0-0) should be of opposite sign. To explain the results of this study, we have to tentatively assign the strong negative band 3 for the three chlorins as Q_x(0-0) because it is the closest band with negative sign to the Q_y(0-0) (band 1) and exhibits a simultaneous change with Q_y(0-0).

3.3. Alcohol and THF treatments of chlorosomes

Fig. 8 shows the absorption and MCD spectra of untreated chlorosomes and chlorosomes treated by hexanol. In the untreated chlorosomes (the dotted line in Fig. 8), the Q_y(0-0) transition is red-shifted to 740 nm and has a broad and small MCD band, implying aggregations of BChl *c* in chlorosomes [18].

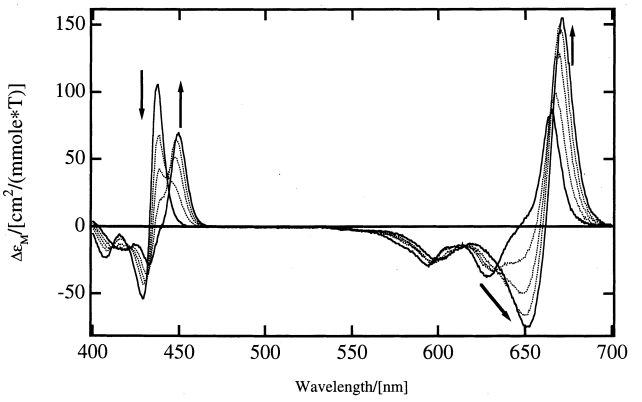

Fig. 7. Titration MCD spectra of BChl *c*/diethyl ether solution by pyridine. The concentration of BChl *c* was calculated as 7.8×10^{-6} mol/l. The volumes of pyridine added into 2 ml diethyl ether were 0, 20, 50, 100 and 250 μl.

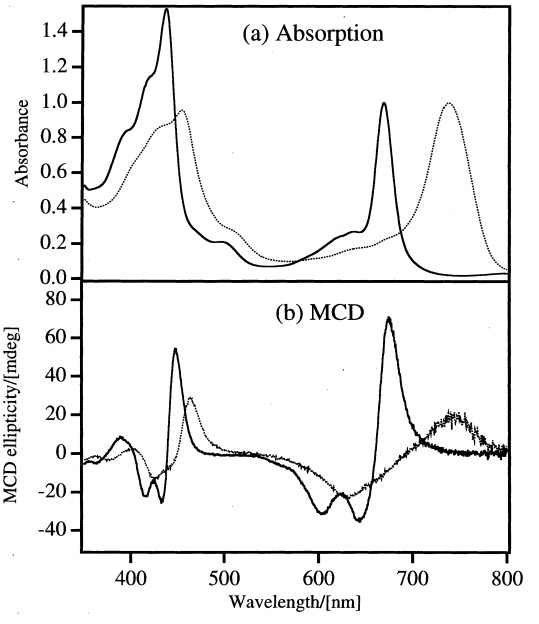

Fig. 8. Absorption (a) and MCD (b) spectra of untreated chlorosomes (dotted lines) and chlorosomes treated with 59 mM hexanol (dotted lines). Concentrations of chlorosomes correspond to the absorbance of 1.0 for the Q_y(0-0) band.

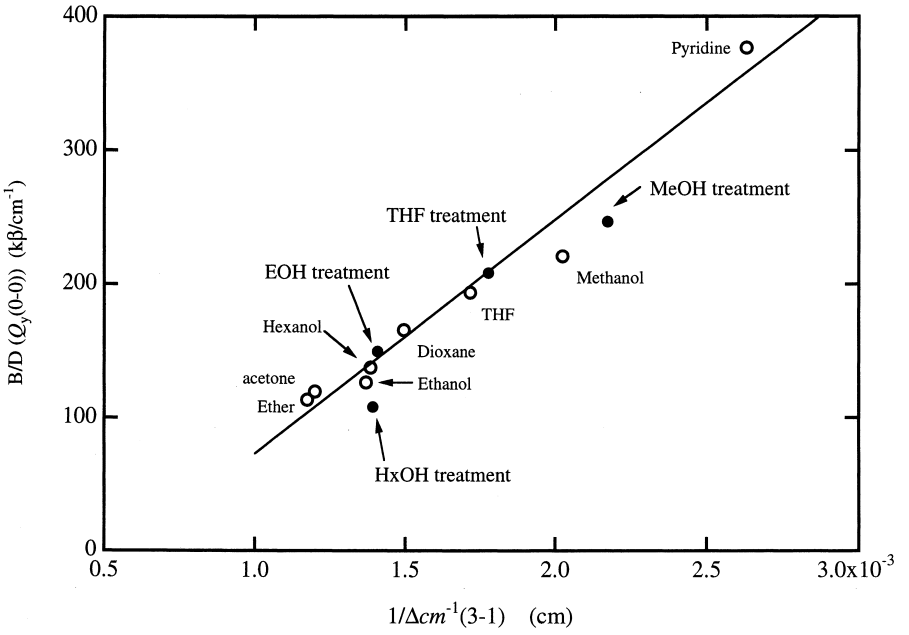

Fig. 9. Correlation between $B/D(Q_y(0\text{-}0))$ and $1/\Delta cm^{-1}(3-1)$ for BChl *c* in various solvents and chlorosomes treated with alcohols and THF. The solid line is the least squares line for BChl *c* in organic solvents. The concentrations of the organic solvents in 20 mM potassium phosphate buffer is as follows: methanol: 17 M, ethanol: 9.5 M, hexanol: 59 mM, THF: 4 M.

With the treatment of hexanol, the absorption and MCD spectra became of the same shapes as those for monomeric BChl *c* (the solid line in Fig. 8). Similar results were observed in treatments with methanol, ethanol and THF. The results were plotted on the map of the correlation between *B*/*D* and energy difference of BChl *c* (Fig. 9). The points of each treatment were located closely to those of BChl *c* in the solvents used in the treatments of chlorosomes, respectively. This indicates that the spectroscopic changes of chlorosomes to monomeric ones are due to the ligation of organic solvent molecules to the Mg atom of BChl *c*. However, the value of *B*/*D* for the hexanol treatment seems to be a little smaller than that of BChl *c* in hexanol. This may indicate that some interactions among BChl *c* molecules still remain in the hexanol-treated chlorosomes as mentioned later.

4. Discussion

The present MCD study on the three intact photosynthetic pigments provided abundant information on the interaction between Mg-chlorin derivatives and various solvents. The results of this study can only be interpreted by assigning the first negative band (band 3), rather than the second negative band (band 5), as being the $Q_x(0\text{-}0)$ transition. Based on such an assignment, the coordination state and the interaction between each pigment and solvent molecules can be well characterized in terms of *B*/*D* value and difference in the transition energy between $Q_y(0\text{-}0)$ and $Q_x(0\text{-}0)$. From a theoretical consideration, the Faraday *B*-term is mainly contributed from mixing of two excited states, S_1 and S_2, and is proportional to the imaginary part of the expression [36]

$$\frac{\langle S_1|m|S_2\rangle\times\langle S_1|\mu|S_0\rangle\times\langle S_2|\mu|S_0\rangle}{E_2-E_1} \quad (1)$$

where S_0, S_1 and S_2 represent the wave functions of the ground and first two excited states, respectively, μ is the electric transition dipole operator, m is the magnetic transition dipole operator, and E_1 and E_2 are the energies of the first two excited states relative to the ground state. The magnitude of the cross-product vector is maximum when the transition dipoles are perpendicular to one other, and otherwise it would become zero if one transition dipole was rotated in a direction parallel to the second transition

dipole. Applying the formula to Q_y(0-0) bands, the *B*/*D* value can be approximately expressed by the following equation:

$$\frac{B(Q_y)}{D(Q_y)} = B_0 + \frac{B_1}{E_x - E_y}\sqrt{\frac{D(Q_x)}{D(Q_y)}} \quad (2)$$

where B_0 and B_1 are constants and D denotes the absorption dipole strength. For BChl *c* in organic solvents, the least squares line for BChl *c* in Fig. 6 was as follows:

$$\frac{B(Q_y)}{D(Q_y)} = -1.02\times10^2 + \frac{1.75\times10^5}{\Delta cm^{-1}} \quad (3)$$

Here Δcm^{-1} is the difference of wave number between Q_x(0-0) (band 3) and Q_y(0-0) (band 1). The correlation coefficient *R* was 0.969. Whereas, taking the change of $(D(Q_x)/D(Q_y))^{1/2}$ into consideration, that line for BChl *c* in organic solvents was drawn as follows:

$$\frac{B(Q_y)}{D(Q_y)} = 4.70 + \frac{1.68\times10^5}{\Delta cm^{-1}}\sqrt{\frac{D(Q_x)}{D(Q_y)}} \quad (4)$$

The value of *R* was 0.976, thus the correlation was also good. It was found that the *B*/*D* value was predominated by the difference of the transition energy and the correlation was only slightly modified by the factors of $(D(Q_x)/D(Q_y))^{1/2}$.

Both Chl *a* and BChl *c* have been identified as five-coordinate species in ether and acetone, and six-coordinate species in THF, methanol and pyridine by resonance Raman measurements [8,11,12,14]. The results of this study show that the coordination number can also be distinguished by analyzing the MCD spectra. Further, more details on the interaction between the pigment and solvent molecules can be obtained from such analysis. Among these solvents, pyridine is the strongest ligand as characterized by a high donor number of 33.1, whereas diethyl ether and acetone are weak ligands with low donor numbers of 19.2 and 17.0 [37]. In the case of BChl *c*, the two groups of solvents are shown to locate at the two sides of the plot in Fig. 6, and other solvents fall between the two extremes due to the variation of the energy difference between Q_y(0-0) and Q_x(0-0), indicating that these solvents could be regarded as ligands with intermediate strength of coordination. This may be useful because it can distinguish the degree of interaction between the pigment and solvent molecule even with the same coordination number, e.g., in the case of THF, methanol and pyridine.

The absorption spectrum of BChl *c* in 1,4-dioxane revealed a split around 610 nm (data not shown), and it was estimated as a six-coordinate-like species [34]. The energy difference between Q_y(0-0) and Q_x(0-0) for dioxane was larger (669 cm^{-1}) than that of THF (582 cm^{-1}), indicating that dioxane may be a weaker ligand than other six-coordinate ligands, THF, methanol and pyridine. A similar analysis was extended to the MCD spectra of several alcohols with longer chains: 1-*n*-propanol, 1-*n*-butanol and 1-*n*-hexanol. It was found that the *B*/*D* values for these solvents located closely to that of ethanol in Fig. 6. Since Chl *a* has been identified as a five-coordinate species in ethanol by resonance Raman [8], BChl *c* in alcohols except for methanol may be five-coordinated and there may exist a boundary of five and six coordination between ethanol and dioxane in the plot of Fig. 6.

Considering the relationship between the value of *B*/*D* and the difference of energy with Q_y(0-0) and Q_x(0-0) in diethyl ether, some characteristics in MCD spectra among Chl *a*, BChl *c* and *d* can be explained. The difference of energy for BChl *c* is smaller than those of Chl *a* and BChl *d* in diethyl ether (Chl *a*: 1012 cm^{-1}, BChl *d*: 931 cm^{-1}, BChl *c*: 855 cm^{-1}), so that in BChl *c* the mixing of band 1 (Q_y(0-0)) and 3 (Q_x(0-0)) becomes larger. Hence, the MCD intensity of band 3 can be stronger than that of band 5 in BChl *c*. It is of interest to note that despite the difference in the absorption maxima, Chl *a* and BChl *d* exhibit similar features in MCD spectra and the *B*/*D* values locate close to each other in the same solvent (Fig. 6). The cause for the difference of energy among pigments in the same solvents may be due to their peripheral substituents. The common structural feature of the two pigments different from BChl *c* is the lack of a 20^1-methyl group. A recent X-ray crystallographic study on methyl ester of (20-methyl phytochlorinato)nickel(II), an analogue of BChl *c*, demonstrated that the structure of this compound has a S_4-ruffled conformation with a higher degree of conformational distortion at the methyl-substituted C20 position [38]. The existence of a 20^1-meth-

yl group could induce a locally steric strain on the neighboring pyrrole rings and eventually cause a highly non-planar macrocycle conformation. Combining the results of this study, we infer that the methylation at the C20 position might play a more important role in the spectral behavior than the substituents at C3, C13[2] positions and the esterifying group.

The assignment of the Q_x(0-0) MCD band for the three chlorin derivatives of this study was different from that made by Houssier and Sauer [15]. In the case of Chl *a* in diethyl ether, they assigned the absorption peak around 614 nm and the first negative MCD peak at 618 nm as Q_y(1-0) and the second negative band at 575 nm as Q_x(0-0). This difference may come from the number of components the absorption peak around 614 nm contains (whether one or two bands). The existence of a peak between the Q_y(0-0) and Q_y(1-0) bands in the fluorescence excitation spectrum of Chl *a* has been observed in diethyl ether at 77 K, with a polarization direction different from that of Q_y(0-0) and Q_y(1-0) [6], and a similar result was obtained in ethanol at 77 K, and in a solution composed of 20% *n*-propyl ether, 40% propane, and 40% propene (in volume) at 75 K [39]. Fragata et al. [40] investigated the spectra mainly by linear dichroism (LD) spectra of Chl *a* oriented in a lamellar phase of glycerylmonoctanoate/H_2O and indicated that there was an *x*-polarized transition between Q_y(0-0) and Q_y(1-0). Therefore, it can be said that there exists an *x*-polarized transition in the absorption peak around 614 nm. If one assigns band 3 as Q_y(1-0), the intensity of Q_y(0-0) should show no simultaneous change with band 3 according to Eq. 1 and Condon approximation. Hence, it is reasonable to assign band 3 as Q_x(0-0) and band 4 as the vibration mode of Q_y(0-0). Keegan et al. [25] reported that the ligation of pyridine increases the energy of the next HOMO for chlorins. We have performed a molecular orbital calculation (data not shown), and also found that the increase in the energy in the next HOMO was larger than that in other MOs (HOMO, LUMO, next LUMO). The lowest energy Q_y(0-0) transition can be described predominantly as a simple one-electron promotion from HOMO to LUMO, while the second lowest energy Q_x(0-0) transition is a mixture of two one-electron promotions, next HOMO to LUMO, and HOMO to next LUMO [36,41]. This may account, at least partly, for a decrease in the spacing between Q_y(0-0) and Q_x(0-0) transitions, because the decrease in transition energy of the Q_x(0-0) transition by coordination is relatively larger than that of the Q_y(0-0).

From this MCD study, it was suggested that the spectroscopic changes of chlorosomes by organic treatments are considered to be due to the ligation of organic solvent molecules to the Mg atom of BChl *c* in chlorosomes. From Fig. 9, the Mg atoms of BChl *c* in chlorosomes are shown to be six-coordinated in the methanol and THF treatments, and five-coordinated in the ethanol and hexanol treatments. Recently, the morphological changes of chlorosomes by hexanol treatment have been reported [31,42]. With electron microscopy and dynamic light scattering measurements, it was observed that the size and shape of chlorosomes were significantly changed during the process of hexanol treatment; the size became large and the shape changed from a rice-grain shape to a stick-like form. However, the glycolipid monolayer on chlorosomes was not broken by hexanol treatment and most BChl *c* molecules were considered to be still confined in the chlorosome particles. We suggested previously that penetration of hexanol molecules through the chlorosome envelope might occur and result in a coordination of the hydroxyl group of hexanol to the Mg atom of BChl *c*. These facts were also pointed out by Zhu et al. [42], Brune et al. [43] and Matsuura et al. [44]. The MCD results support that hexanol molecules dissociate the BChl *c* aggregates by coordinating to the Mg atom in the fifth position after penetration into chlorosomes. The value of *B*/*D* after hexanol treatment seems to be a little smaller than that of BChl *c* in hexanol. The value of *B*/*D* depends not only on the difference in energy of Q_x(0-0) and Q_y(0-0) but also on the aggregation of pigments [18]. The formation of aggregate leads to a decrease in the value of *B*/*D*, which is considered to be due to interaction among pigments. The value of the dimer of BChl *a* is half that of the monomer [18]. The energy difference is determined by the coordinate state of the Mg atom. The energy difference between Q_x(0-0) and Q_y(0-0) for chlorosomes treated by hexanol was about the same as that of BChl *c* in hexanol (see the value of the abscissa in Fig. 9). Therefore this little decrease may attribute to a weak interaction between pigments

and indicate that complete dissociation of BChl *c* aggregates in chlorosomes does not happened. Penetration and ligation of water molecules may be considered. However, we think that the inside of chlorosomes is very hydrophobic. The penetration of water into chlorosomes would need much more energy.

In conclusion, the MCD spectra of Chls in the visible region were sensitive to the coordination state of pigment by various solvent molecules. The interaction between pigment and solvent can be characterized in terms of the relationship between *B*/*D* values of Q_y(0-0) and the difference in energies of Q_x(0-0) and Q_y(0-0) transitions. This correlation is very useful to determine not only the coordination number of the central metal atom of pigments but also the relative bonding power of solvents. With this new technique, it can be shown that the spectroscopic changes of chlorosomes by alcohol and THF treatments are due to the ligation of organic solvent molecules to the Mg atom of BChl *c* in chlorosomes.

Acknowledgements

We are grateful to Prof. Mamoru Mimuro, Dr. Toru Oba and Yukio Imamura for discussion about Chl *a* and chlorosomes. This work was supported by Grants-in-Aid from the Ministry of Education, Science and Culture, Japan (Nos. 06555257, 07455437, 07750872, 08455377).

References

[1] J.J. Katz, M.K. Bowan, T.J. Michalski, D.L. Worcester, in: H. Scheer (Ed.), Chlorophylls, CRC Press, Boca Raton, FL, 1991, pp. 211–236.
[2] R.E. Blankenship, J.M. Olson, M. Miller, in: R.E. Blankenship, M.T. Madigan, C.E. Bauer (Eds.), Anoxygenic Photosynthetic Bacteria, Kluwer Academic Publishers, Dordrecht, 1995, pp. 399–435.
[3] K. Ballschmiter, J.J. Katz, J. Am. Chem. Soc. 91 (1969) 2661–2677.
[4] J. Chiefari, K. Griebenow, T.S. Balaban, A.R. Holzwarth, K. Schaffner, J. Phys. Chem. 99 (1995) 1357–1365.
[5] K. Sauer, J.R.L. Smith, A. Schultz, J. Am. Chem. Soc. 88 (1966) 2681–2688.
[6] L.L. Shipman, T.M. Cotton, J.R. Norris, J.J. Katz, J. Am. Chem. Soc. 98 (1976) 8222–8230.
[7] T.M. Cotton, R.P.V. Duyne, J. Am. Chem. Soc. 103 (1981) 6020–6026.
[8] M. Fujiwara, M. Tasumi, J. Phys. Chem. 90 (1986) 250–255.
[9] M. Fujiwara, M. Tasumi, J. Phys. Chem. 90 (1986) 5646–5650.
[10] G.A. Schick, D.F. Bocian, Biochim. Biophys. Acta 895 (1987) 127–154.
[11] M. Lutz, G.V. Van Braket, in: Green Photosynthetic Bacteria, Plenum Press, New York, 1988, pp. 23–34.
[12] T. Nozawa, T. Noguchi, M. Tasumi, J. Biochem. 108 (1990) 737–740.
[13] P. Hildebrandt, H. Tamiaki, A.R. Holzwarth, K. Schaffner, J. Phys. Chem. 98 (1994) 2192–2197.
[14] H. Sato, K. Uehara, T. Ishii, Y. Ozaki, Photochem. Photobiol. 62 (1995) 509–513.
[15] C. Houssier, K. Sauer, J. Am. Chem. Soc. 92 (1970) 779–791.
[16] D. Frackowiak, D. Bauman, H. Manikowski, W. Browett, M. Stillman, Biophys. Chem. 28 (1987) 101–114.
[17] S. Choi, J.A. Phillips Jr., W. Ware, C. Wittschieben, C.J. Medforth, K.M. Smith, Inorg. Chem. 33 (1994) 3873–3876.
[18] M. Kobayashi, Z.-Y. Wang, K. Yoza, M. Umetsu, H. Konami, M. Mimuro, T. Nozawa, Spectrochim. Acta Part A 51 (1996) 585–598.
[19] Y. Nonomura, S. Igarashi, N. Yoshioka, H. Inoue, Chem. Phys. 220 (1997) 155–166.
[20] T.A. Evance, J.J. Katz, Biochim. Biophys. Acta 396 (1975) 414–426.
[21] M. Gouterman, in: D. Dolphin (Ed.), The Porphyrins, vol. III, Academic Press, New York, 1978, pp. 1–165.
[22] P.J. Stephens, J. Chem. Phys. 52 (1970) 3489–3516.
[23] J. Michl, J. Am. Chem. Soc. 100 (1978) 6801–6811.
[24] J.D. Keegan, A.M. Stolzenberg, Y.-C. Lu, R.E. Linder, G. Barth, A. Moscowitz, E. Bunnenberg, D. Djerassi, J. Am. Chem. Soc. 104 (1982) 4305–4317.
[25] J.D. Keegan, A.M. Stolzenberg, Y.-C. Lu, R.E. Linder, G. Barth, A. Moscowitz, E. Bunnenberg, D. Djerassi, J. Am. Chem. Soc. 104 (1982) 4317–4329.
[26] L.A. Staehelin, J.R. Golecki, R.C. Fuller, G. Drews, Arch. Mikrobiol. 119 (1978) 269–277.
[27] L.A. Staehelin, J.R. Golecki, G. Drews, Biochim. Biophys. Acta 589 (1980) 30–45.
[28] M. Mimuro, T. Nozawa, N. Tamai, K. Shimada, I. Yamazaki, S. Lin, R.S. Knox, B.P. Wittmershaus, D.C. Brune, R.E. Blankenship, J. Phys. Chem. 93 (1989) 7503–7509.
[29] A.R. Holzwarth, K. Griebenow, K.Z. Schaffner, Naturforschung 45c (1990) 203–206.
[30] K. Griebenow, A.R. Holzwarth, F. van Mourik, R. van Grondelle, Biochim. Biophys. Acta 1058 (1991) 194–202.
[31] Z.-Y. Wang, G. Marx, M. Umetsu, M. Kobayashi, M. Mimuro, T. Nozawa, Biochim. Biophys. Acta 1232 (1995) 187–196.
[32] T. Omata, N. Murata, Biochim. Biophys. Acta 501 (1978) 103–111.
[33] T. Nozawa, M. Suzuki, K. Ohtomo, Y. Morishita, H. Konami, M.T. Madigan, Chem. Lett. (1991) 1641–1644.

[34] G.R. Seely, R.G. Jensen, Soectrochim. Acta 21 (1965) 1835–1845.
[35] R.J. Porra, in: H. Scheer (Ed.), Chlorophylls, CRC Press, Boca Raton, FL, 1991, p. 54.
[36] J.C. Sutherland, J.M. Olson, Photochem. Photobiol. 33 (1981) 379–384.
[37] V. Gutmann, in: The Donor-Acceptor Approach to Molecular Interactions, Plenum Press, New York, 1978, Ch. 2.
[38] M.O. Senge, K.M. Smith, Photochem. Photobiol. 60 (1994) 139–142.
[39] S. Freed, K.M. Sancier, Science 114 (1951) 275–276.
[40] M. Fragata, B. Norden, T. Kurucsen, Photochem. Photobiol. 47 (1988) 133–143.
[41] J.D. Petke, G.M. Maggiora, L. Shipman, R.E. Christoffersen, Photochem. Photobiol. 30 (1979) 203–223.
[42] Y. Zhu, B.L. Ramakrishna, P.I. van Noort, R.E. Blankenship, Biochim. Biophys. Acta 1232 (1995) 197–207.
[43] D.C. Brune, T. Nozawa, R.E. Blankenship, Biochemistry 26 (1986) 8644–8652.
[44] K. Matsuura, J.M. Olson, Biochim. Biophys. Acta 1019 (1990) 233–238.